

# ***In Vivo* and *Ex Vivo* Inhibition of Spinal Nerve Ligation-Induced Ectopic Activity by Sodium Channel Blockers Correlate to *In Vitro* Inhibition of NaV1.7 and Clinical Efficacy: A Pharmacokinetic-Pharmacodynamic Translational Approach**

Ivana Kalezić · Lei Luo · Per-Eric Lund · Anders B Eriksson · Tjerk Bueters · Sandra A. G. Visser

Received: 21 September 2012 / Accepted: 7 January 2013 / Published online: 1 February 2013  
© Springer Science+Business Media New York 2013

## **ABSTRACT**

**Purpose** *In vivo* and *ex vivo* inhibition of ectopic activity of clinically used and newly developed sodium channel (NaV) blockers were quantified in the rat spinal nerve ligation (SNL) model using a pharmacokinetic-pharmacodynamic (PKPD) approach and correlated to *in vitro* NaV1.7 channel inhibition and clinical effective concentrations.

**Methods** *In vivo*, drug exposure and inhibition of ectopic activity were assessed in anaesthetized SNL rats at two dose levels. *Ex vivo*, compounds were applied at increasing concentrations to dorsal root ganglia isolated from SNL rats. The inhibitory potency ( $IC_{50}$ ) was estimated using PKPD analysis. *In vitro*  $IC_{50}$  was estimated using an electrophysiology-based assay using recombinant rat and human NaV1.7 expressing HEK293 cells.

**Results** *In vivo* and *ex vivo* inhibition of ectopic activity correlated well with the *in vitro* inhibition on the rat NaV1.7 channel. The estimated  $IC_{50}$ s for inhibition of ectopic activity in the SNL model occurred at similar unbound concentrations as clinical effective concentrations in humans.

**Conclusions** Inhibition of ectopic activity in the SNL model could be useful in predicting clinical effective concentrations for novel sodium channel blockers. In addition, *in vitro* potency could be used for screening, characterization and selection of compounds, thereby reducing the need for *in vivo* testing.

**KEY WORDS** ectopic activity · NaV1.7 · pharmacokinetics and pharmacodynamics · sodium channels · spinal nerve ligation rat model

## **ABBREVIATIONS**

ACSF	artificial cerebral spinal fluid
$C_e$	concentration in the biophase
CIP	congenital insensitivity to pain
$C_p$	concentration in plasma
DRG	dorsal root ganglion
$E$	effect at a certain concentration
$E_0$	baseline of effect
$E_{max}$	maximal attainable effect
i.v	intravenous
$IC_{50}$	concentration at which 50% inhibition is achieved
$k_{eo}$	rate constant between plasma and biophase concentration
LC-MS/MS	liquid chromatography with mass spectrometry detection
$n$	hill slope factor
NaV	voltage-gated sodium channel
PKPD	pharmacokinetic-pharmacodynamic
SNL	spinal nerve ligation

**Electronic supplementary material** The online version of this article (doi:10.1007/s11095-013-0979-6) contains supplementary material, which is available to authorized users.

I. Kalezić · L. Luo · P.-E. Lund · A. B. Eriksson  
Neuroscience, CNSP Innovative Medicines  
AstraZeneca R&D  
S-151 85, Södertälje, Sweden

T. Bueters  
DMPK, CNSP Innovative Medicines  
AstraZeneca R&D  
S-151 85, Södertälje, Sweden

S. A. G. Visser (✉)  
Global DMPK, Centre of Excellence  
Innovative Medicines, AstraZeneca R&D  
SE-151 85, Södertälje, Sweden  
e-mail: sagvisser@yahoo.com

## INTRODUCTION

Neuropathic pain, such as spinal nerve root pain, pain after nerve trauma, diabetic neuropathy, and pain after shingles, is a heterogeneous group of disorders with various nerve injuries as the underlying cause of pain. There is a large unmet need for effective and safe treatment of neuropathic pain (1). Sodium channel blockers with low potency, such as lidocaine, mexiletine, carbamazepine, and tricyclic antidepressants like amitriptyline have been reported to have effect against neuropathic pain (2, 3). However, severe CNS- and/or CV-related adverse effects limit their clinical utility due to poor selectivity *versus* physiologically important sodium channels or unfavorable brain distribution (4).

In humans, the voltage-gated sodium channel (NaV) family consists of nine distinct subtypes (NaV1.3, NaV1.7, NaV1.8 and NaV1.9), which are thought to play a role in pain signaling (4). NaV1.7 is perhaps the best validated pain target of these channels based on evidence from human genetic studies. In Congenital Insensitivity to Pain (CIP) patients that lack a functional NaV1.7 channel, complete pain insensitivity is observed. Apart from that, these patients have a normal phenotype including feeling of touch and cold and warm temperature (5, 6). In contrast, severe pain is associated with gain of function mutations in the NaV1.7 channel in patients with Erythromelalgia or Paroxysmal Extreme Pain Disorder, (7, 8).

Large investments in drug discovery are being made to develop more potent and/or more selective sodium channel blockers aiming to improve the overall therapeutic profile of this class of drugs by limiting the side effect potential (1, 4, 9, 10). One challenge to overcome is the projection of the required pharmacokinetic profile to elicit meaningful pain alleviation over a prolonged time in human for such new chemical entities. This requires an understanding of the compound's potency and intrinsic activity, time course of the effect, and dose and time dependencies in a relevant preclinical disease model, which is translatable to the human clinical setting (11, 12). Therefore, linking the preclinical effects of available sodium channel blockers to their clinical efficacy is instrumental in understanding the utility of preclinical models in the translation to the clinical setting for novel compounds.

*In vivo* electrophysiology recording of ectopic discharges over time could potentially be a suitable pharmacodynamic endpoint to study the pharmacokinetic-pharmacodynamic (PKPD) properties of drugs, because the effect and exposure can be measured repeatedly over time in the same animal. Such experimental design allows quantification of the time-course of effect based on the plasma concentration and the *in vivo* potency for each compound (13). Effects on nerve ligation-induced ectopic activity have previously been demonstrated for several of sodium channel blockers (14–18).

However, since the *in vivo* inhibitory potencies were not reported, the translational value of this endpoint remains difficult to assess.

In the present investigation we quantified the *in vivo* and *ex vivo* inhibition of ectopic activity of clinically used as well as in-house developed sodium channel blockers in the rat spinal nerve ligation (SNL) model using a PKPD translational approach. It was investigated if the *in vivo* and *ex vivo* inhibition correlated to the *in vitro*  $IC_{50}$  obtained in the electrophysiology assay using rat NaV1.7 expressing HEK293 cells. In addition, for clinically used sodium channel blockers, it was studied if *in vivo* inhibition of ectopic activity in rats was correlated to clinically effective plasma concentrations.

## MATERIALS AND METHODS

### Chemicals

All compounds were synthesized internally at the Department of Medicinal Chemistry at AstraZeneca R&D Södertälje with the exception of amitriptyline, carbamazepine, lamotrigine, mexiletine, and tetracaine, which were purchased from Sigma-Aldrich (St. Louis, MO, USA). Some of the structures have recently been published in the scientific or patent literature. AZ-9 belongs to a chemical series of phenyl isoxazoles and corresponds to compound 24 (19), AZ-10 and AZ-19 belong to the chemical series of phenethyl nicotinamides and correspond to compound 6 and 3, respectively (20), AZ-3 and AZ-8 belong to the N-chroman-3-ylcarboxamide series and correspond to compound 13 and 15, respectively (21). AZ-16 belongs to a series of 3-oxoisindoline-1-carboxyamides and corresponds to compound 28B (22). Finally, AZ-17 and AZ-20 belong to the same chemical series of sulphonamides (23).

### Animals and Spinal Nerve Ligation (SNL) Surgery

The experimental procedures followed the guidelines and recommendations of Swedish Animal Protection Legislation and were approved by the South Stockholm Committee for Ethical Experiments on Laboratory Animals.

Adult male Sprague–Dawley rats (Harlan Laboratories B.V, Holland), weighing 125–150 g, were housed in groups of 3 in plastic cages with the floor covered with soft sawdust bedding under a 12 h light/12 h dark cycle (lights on 06:00 h). They were kept in a room at a constant ambient temperature. Water and food were supplied *ad libitum*. The rats were habituated for at least 7 days before experimental manipulations. The SNL surgery was done according to the method described by Liu *et al.*, (24). Briefly, rats were anesthetized with a mixture of isoflurane (5% for induction and

3% for maintenance) and a 2:1 flow of O<sub>2</sub> and air, the left L5 (and occasionally L4) spinal nerves were exposed and ligated tightly with 6–0 silk threads. Wounds were closed and anesthesia was discontinued. Animals were kept on a warm plate until they completely recovered from anesthesia and resumed normal activities.

### In Vivo Electrophysiology

On average 2 weeks following SNL surgery rats were re-anesthetized and artificially ventilated with a mixture of isoflurane (5% to 3.5%), air and O<sub>2</sub>. The weight of the animals was between 280 and 320 g at start of the experiment. Catheters were inserted into the right jugular vein for drug administration. ECG and heart rate were monitored. Body core temperature was kept at physiological level (37–38°C) using a feedback-controlled radiant heater. The level of anesthesia was monitored by checking the withdrawal and corneal reflexes. The cauda equina was exposed in a lower lumbar laminectomy, the dura was open and dorsal roots L3–L6 were separated. The exposed neural tissue was covered in warm paraffin oil (34°C).

Spontaneous activity originating in dorsal root ganglion (DRG) neurons and neuroma was recorded from microfilaments, which were cut centrally but in continuity with DRG distally and separated from the dorsal root near its point of entry into the spinal cord, 16–31 mm central to the DRG. The transected ends of the microfilaments were placed on bipolar, platinum electrodes. Each microfilament was observed passively for < 2 min. If no activity was found during this period, a new filament was inserted. Microfilaments often contained more than one spontaneously active axon (unit). Different active axons were discriminated based on their spike amplitude and waveform by monitoring the spike waveform continuously using a delay line and window amplitude discriminator (Spike2 v5.01, Cambridge Electronic Design (CED), UK). Two to four units in a filament were acceptable if they were readily distinguishable throughout the course of the experiment. The spike waveforms and firing patterns were recorded and displayed as raw data and peri-stimulus time histograms. Inter-spike interval histograms (estimated from 50 and 100 s recorded segment) were also made revealing the differences in action potential spacing in recorded spontaneously active neurons with different patterns.

Once stable baseline activity was recorded for a 5–10 min period, a compound was infused intravenously for 20 min followed by a washout period of 30 min. Recordings were made continuously during the whole time-course of the experiment. Each compound was studied at two dose levels for 6–8 recordings. In each experiment correction for cannulae volume was performed (0.05 ml). The estimated delay from infusion pump to animal was 2 min. At two occasions

(5 or 10 min after cessation of the infusion and at the end of the experiment) blood samples were collected for analysis of the plasma concentration. Exact time of sampling was noted and used in the data-analysis.

The action potentials and ECG were amplified using amplifiers: Cyber Amp Signal Conditioner 380 (Axon Instrument, USA) or DAM50 (WPI Inc, USA) and Iso-Dam 8 modules (WPI Inc, USA). The frequency bandwidth for the spontaneous action potentials and ECG was set to a range of 10 Hz to 10 kHz. Signals were sampled by CED Power 1401 (CED, UK) and analyzed with Spike2 software (CED, UK). The input signals were digitized with 12-bit resolution at rates of 1 kHz for ECG and 15 kHz for spikes. The data analysis was performed using the Origin 7.0 software (OriginLab Corporation, USA).

Ectopic activity was not uniform from the individual afferent fibres, which all have their own intrinsic physiological characteristics. They could differ between each other in discharge frequency and pattern of activity. To standardize their response it was necessary to normalize their discharge frequency in distinct time intervals during compound infusion to the spontaneous control frequency. For individual fiber, mean frequency during control period and each successive time interval (5 min duration) was quantified using peristimulus time histograms (number of spikes occurring per 1-s bin). The value for each interval was then normalized to the change from the mean control frequency before infusion. The magnitude and time profile of inhibition were calculated. A fiber was responsive if the reduction of its firing frequency during and after the end of infusion exceeded mean  $\pm$  2 standard deviation of the control frequency. Inhibitory effects from population of observed fibres were measured and expressed as mean  $\pm$  standard error of mean (SEM).

### Ex Vivo Electrophysiology

The experimental procedures for *ex vivo* electrophysiology have been described in detail elsewhere (22). In brief, 3 to 9 days after SNL surgery, animals were anesthetized with isoflurane. The DRG with attached dorsal roots and spinal nerve stumps were mounted in a chamber. The DRG and spinal nerve compartments were perfused with oxygenated artificial cerebrospinal fluid (ACSF) at a rate of 1.25–1.5 ml/min. The temperature was kept at  $35 \pm 0.5^\circ\text{C}$ . Single fiber recordings were performed, and ectopic discharges were recorded from teased dorsal root fascicles. Once stable baseline of ectopic discharge was established and recorded for at least 5 min, ACSF followed by three concentrations of a single compound were applied cumulatively to the DRG compartment for 10–15 min via a pump, at a rate of 1.25–1.5 mL/min. In the experiments, three concentration levels were used corresponding to 1, 3, and 10 times of the  $IC_{50}$

value in the NaV1.7 *in vitro* assay. The ectopic activities during application of buffer (ACSF) and drugs were averaged every 3 min and then normalized to the percentage change of mean control frequency. The magnitude and time profile of inhibition were calculated. Data are expressed as mean  $\pm$  SEM.

### IonWorks Quattro Electrophysiological Assay

The recombinant HEK293 cell line stably expressing human NaV1.7 $\alpha$  was obtained from Millipore (Billerica, MA, USA). The rat NaV1.7 cell line was kindly donated by Mohamed Chahine (Department of Medicine and Laval Hospital, Laval University, QC, Canada). Cell lines and culture conditions have been described elsewhere (22). Prior to electrophysiological recordings, the cells were incubated at 30°C during the last 15–24 h, washed with Mg and Ca-free PBS, detached with trypsin, centrifuged and resuspended in D-PBS, and finally added to the Ion Works cell boat at 1.3 billion cells/mL.

Electrophysiological recordings were carried out using the IonWorks Quattro (Molecular Devices LCC, Sunnyvale, CA, US). Principles and operation of the IonWorks Quattro/HT instrument have been described by Schroeder *et al.* (25). The experimental details of the electrophysiology recordings have been described in detail elsewhere (22). In brief, test compounds with a final DMSO concentration of 0.3% were prepared in a 384-well plate (V-bottom, Greiner Bio-One, Kremsmuenster, Austria). The compounds were analyzed using two different voltage protocols. The cells were either clamped to  $-90$  mV, where the majority of channels are in a resting state, or they were clamped to  $-65$  mV, which is referred to as the steady state. The sodium currents were evoked by a single voltage train consisting of eight 30 ms depolarizing steps to  $-20$  mV from the holding potential at a frequency of 3 Hz. To recover a fraction of the channels from slow inactivation with the steady state ( $V_{\text{hold}} -65$  mV) protocol, a 20 ms hyperpolarizing step to  $-100$  mV was executed prior to the activation step. The protocol was activated twice, pre-scan and post-scan compound addition and the degree of inhibition for each well was assessed by dividing the two values for the eight pulses. Currents greater than 0.1 nA after subtraction were included in the analysis, and commonly represent around 80% of all cells recorded from. Statistics was carried out using unpaired students *t*-test, and a  $p < 0.05$ . Concentration-dependent inhibitory curves were constructed to estimate the  $IC_{50}$  of the test compounds. All compounds were analyzed with  $n = 2$ –38 at different test occasions.

### Bioanalysis of Plasma Samples

In the *in vivo* electrophysiology study, 0.4–0.5 ml of blood samples were collected in heparinized tubes. The tubes were

immediately put on iced water and centrifuged at 3000 rpm for 10 min at 4°C, within 1 h after collection. The plasma (0.2 ml) was transferred to a polypropylene tube and frozen immediately at 70°C until analysis. Sample preparation and bioanalysis with LC-MS/MS have been previously described in detail (26, 27).

### Plasma Protein Binding

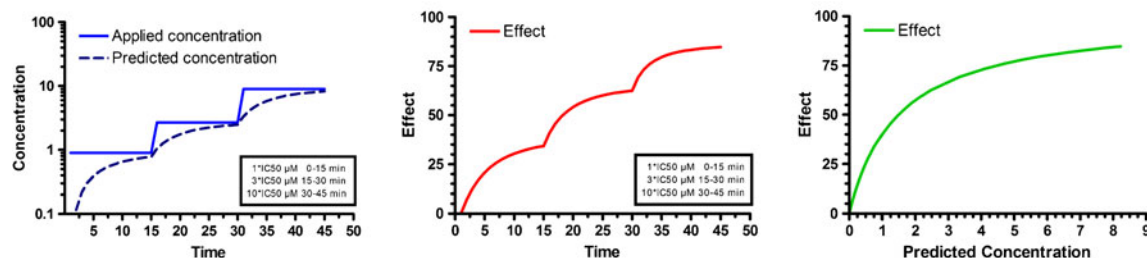
Human plasma (pooled from three individuals) was collected internally at AstraZeneca. Rat plasma was prepared in house from male Sprague–Dawley rats. Plasma protein binding was determined by equilibrium dialysis as described in Borgegård *et al.*, (28). In short, compounds were added to rat and human plasma to a final concentration of 10  $\mu$ M. An aliquot of 180  $\mu$ L was transferred to a dialysis plate with phosphate buffer on the other site and incubated for 18 h at 37°C. Proteins were removed from aliquots (50  $\mu$ L) of plasma and buffer samples, internal standard added, and analyzed with LC-MS/MS. The unbound fraction in plasma was calculated from the ratio of the MS-area of the compound of interest in buffer divided by sum of the areas of the compound in buffer and plasma. Recovery and stability in plasma was controlled for.

### Pharmacokinetic-Pharmacodynamic Analysis

Figure 1 schematically shows the PKPD data-analysis approach. For the *in vivo* electrophysiology results, the pharmacokinetics and pharmacodynamics were quantified in a 2-step approach. First, the pharmacokinetic parameters of all compounds were estimated using a standard 2-compartment pharmacokinetic model. The observed plasma concentrations taken during or shortly after the electrophysiological experiments were not sufficient to fully characterize the pharmacokinetic model. Therefore, we added detailed pharmacokinetic information after routine iv bolus (3  $\mu$ mol/kg) to 3 Sprague Dawley rats to the pharmacokinetic data-analysis. Additional pharmacokinetic data for amitriptyline, lidocaine and mexilitine were used from the literature as listed in Table I.

Data of responding individual fibers were pooled per dose and scaled from 0 to 1, where 0 means no inhibition and 1 means maximal inhibition. Plasma concentrations at each effect observation during the experiment were predicted using the pharmacokinetic parameters. When plotting the plasma concentration *vs* the inhibition of ectopic activity, a hysteresis loop was observed indicating a small time delay between the plasma concentrations and the effect. In the PKPD analysis this was taken into account by applying an effect-compartment model (29). In the effect-compartment approach, it is assumed that the effect is

## Ex-vivo electrophysiology



## In-vivo electrophysiology

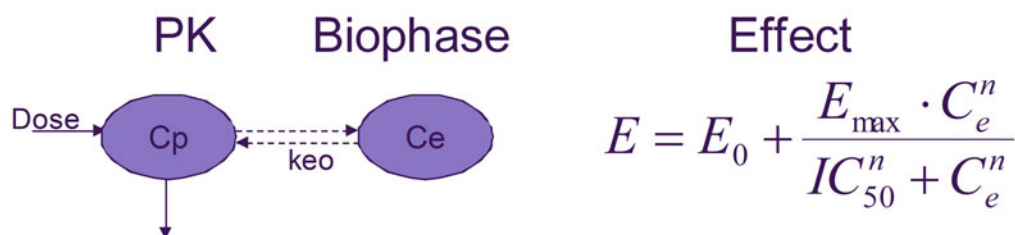
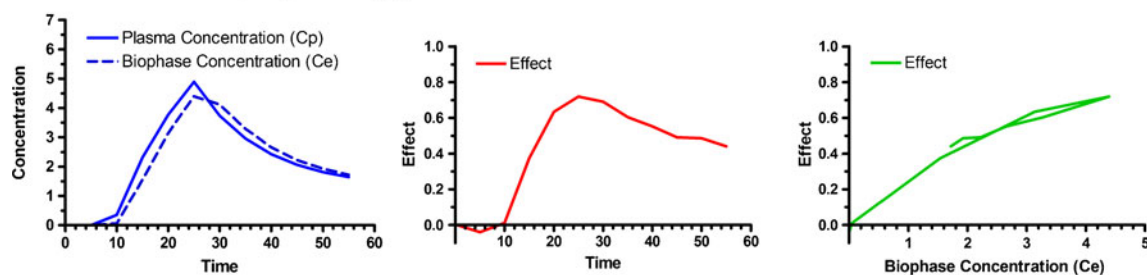


**Fig. 1** Schematic representation of the experimental setup and the pharmacokinetic-pharmacodynamic analysis. *Ex vivo* electrophysiology: the ‘actual’ concentration (dotted line) in the chamber was predicted assuming a 5 min delay of distribution of the applied concentrations in the buffer. This predicted actual concentration was assumed to drive the *ex vivo* effect following a sigmoidal  $E_{\max}$  model. *In vivo* electrophysiology: the biophase concentration (dotted line) was estimated in the PKPD analysis by assuming a direct relationship between biophase concentrations and the effect on ectopic activity (Eqs. 1 and 2). A schematic representation of the pharmacokinetics and distribution to the biophase is shown below the schematic graphs.

**Table 1** Pharmacokinetic Parameter Estimates Derived from a Simultaneous Analysis of Plasma Concentrations After Intravenous Bolus Dose (3  $\mu\text{mol/kg}$ , Data not Shown) and the Plasma Exposure from the *In Vivo* Electrophysiology Study for the Clinically Used Sodium Channel Blockers

Compound	CL (L/h/kg)	$V_1$ (L/kg)	$CL_D$ (L/h/kg)	$V_2$ (L/kg)
Amitriptyline <sup>a</sup>	5.4	0.017	13.5	2.8
Carbamazepine	0.086	1.1	2.2	13
Lamotrigine	0.023	0.95	1.2	0.99
Lidocaine <sup>b</sup>	2.9	0.73	3.3	1.1
Mexilitine <sup>c</sup>	4.2	3.7	7.0	6.8

<sup>a</sup> Additional data from Bae et al., J Pharm Sci 2009 Apr;98(4):1587–1601

<sup>b</sup> Additional data from Supradist et al., J Pharm Pharmacol 1984 Apr;36(4):240–243

<sup>c</sup> Based on data from Nagasako et al. J Pharm Pharmacol 1992 Jan;44(1):55–57

directly related to the concentration of the drug in a hypothetical effect site or so-called biophase ( $C_e$ ).

$$E = E_0 + \frac{E_{\max} \cdot C_e^n}{IC_{50}^n + C_e^n} \quad (1)$$

in which  $E$  is the effect at a certain concentration  $C_e$  in the biophase,  $E_0$  is the baseline activity of the system without drug effect,  $E_{\max}$  is the maximal attainable effect,  $IC_{50}$  is the concentration at which 50% inhibition is achieved and  $n$  is the hill slope factor. The equilibrium rate between plasma and biophase concentrations was described by a rate constant  $k_{eo}$  which describes the delay between plasma and biophase concentrations.

$$\frac{d(C_e)}{dt} = k_{eo} \cdot (C_p - C_e) \quad (2)$$

The following assumptions were made in the PKPD analysis: the pharmacokinetic profile of the compound was



similar for each nerve fiber. Maximal effect was fixed at 1 (i.e., full inhibition possible) and baseline activity of the system without drug presence was fixed at 0 to reduce the numbers of parameters to be characterized. All PKPD modeling was performed using Winnonlin 5.2 (Pharsight Corp. Palo Alto, USA).

## RESULTS

### In Vivo Electrophysiology

Extracellular recordings were made from neurons with tonic discharge pattern in SNL rats using five clinically used drugs; carbamazepine, lidocaine, mexiletine, lamotrigine, and amitriptyline as well as six in house compounds from our NaV1.7 drug discovery program. Inter-spike interval histograms of the spontaneous activity revealed that action potential spacing exhibited a dominant frequency. Neurons with tonic irregular pattern (48/69) had a scatter around the dominant frequency, and the scatter increased as frequencies dropped. Neurons with rhythmic pattern (21/69) displayed less variability in interspike intervals and exhibited metronome-like regularity in action potential spacing. Infusion of saline in control experiments ( $N=3$ ) did not show any significant effect on the firing frequency (data not shown).

An intravenous dose of  $37 \mu\text{mol/kg}$  of lidocaine over 20 min was studied on 9 ectopic units from 8 animal preparations and its effect is shown in Fig. 2 as a typical example. Figure 2a displays a rate meter recording from a spontaneous active neuron isolated from a L5 fibre after SNL. Lidocaine reduced the spontaneous neuronal firing by 80% with maximal inhibition at the end of the infusion. After cessation of the infusion, the firing pattern fully recovered within 10 min. It caused a slight effect on ECG and a transient decrease of  $14 \pm 2\%$  on heart rate. Figure 2b shows the individual response of each of the 9 units analysed. All recorded units had a tonic character and the average maximum inhibitory levels were  $0.48 \pm 0.22$  and  $0.71 \pm 0.12$  for the 2 doses tested. Similar results were observed for the ten other tested compounds.

For each compound, the observed plasma concentrations were fitted simultaneously to a standard 2-compartment pharmacokinetic model together with in house available intravenous bolus data ( $3 \mu\text{mol/kg}$ ) and/or literature data. Pharmacokinetic parameters estimates for the clinically used sodium channel reference compounds are listed in Table I. Pharmacokinetics and pharmacodynamics for lidocaine and AZ-1 are shown in Fig. 3 as typical examples. The pharmacokinetics, pharmacodynamics and the PKPD graphs for the other compounds can be found in the Supplementary Material Figs. S1 and S2. The predicted plasma profiles described the actual measured concentrations with high

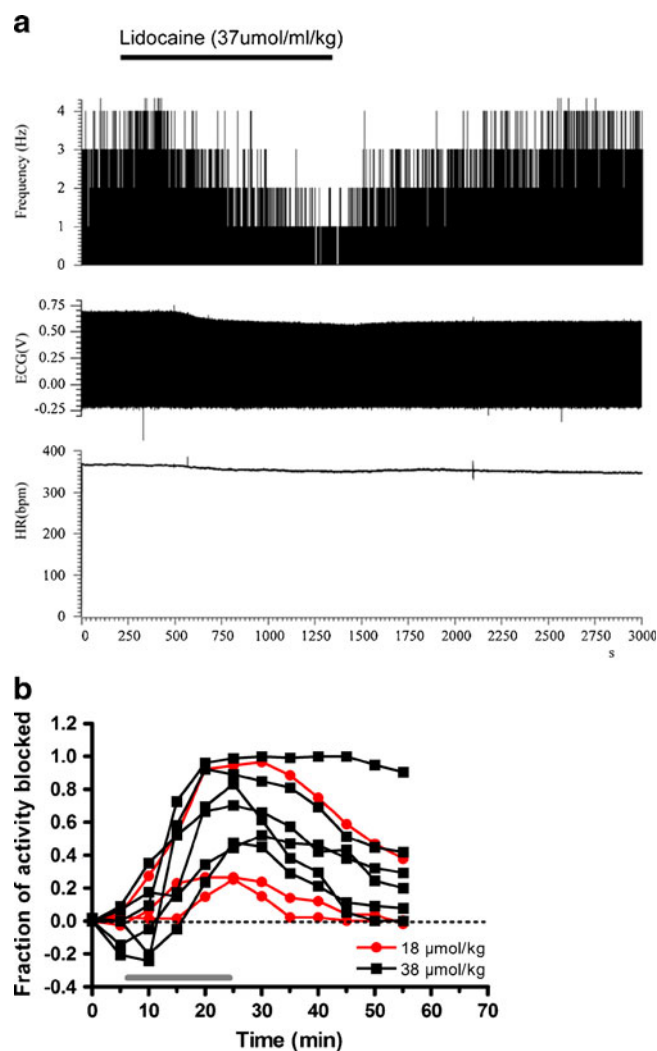


**Fig. 2** (a) Frequency (Hz), ECG (V) and HR (bpm) rate meter recording from a spontaneously active neuron isolated from L5 fibre following spinal nerve ligation during intravenous application of lidocaine at  $37 \mu\text{mol/kg}$  for 20 min. Lidocaine reduced spontaneous activity by 80%, followed by quick recovery. (b) Time-courses of the inhibition of ectopic activity of lidocaine on individual fibres at two dose levels.

accuracy. Plasma concentrations were calculated at each time-point of measurement of ectopic activity. It was observed that the inhibitory effect on ectopic activity was slightly delayed relatively to the plasma concentrations for all tested compounds. Therefore, an effect compartment PKPD model (Eq. 1 and 2) was used to describe the observations and estimate the parameters:  $k_{eo}$ ,  $IC_{50}$  and  $n$ . Ectopic activity in some fibres was completely blocked, which showed that fixing  $E_{max}$  to 100% was justified. The pharmacodynamic parameter estimates for all compounds are listed in Table II. Figure 3 (middle panels) shows that the average time-course profiles of the reduction of ectopic discharges were accurately described by the PKPD model. A full inhibitory curve was constructed from the concentrations in the biophase from both doses and the inhibitory effect on

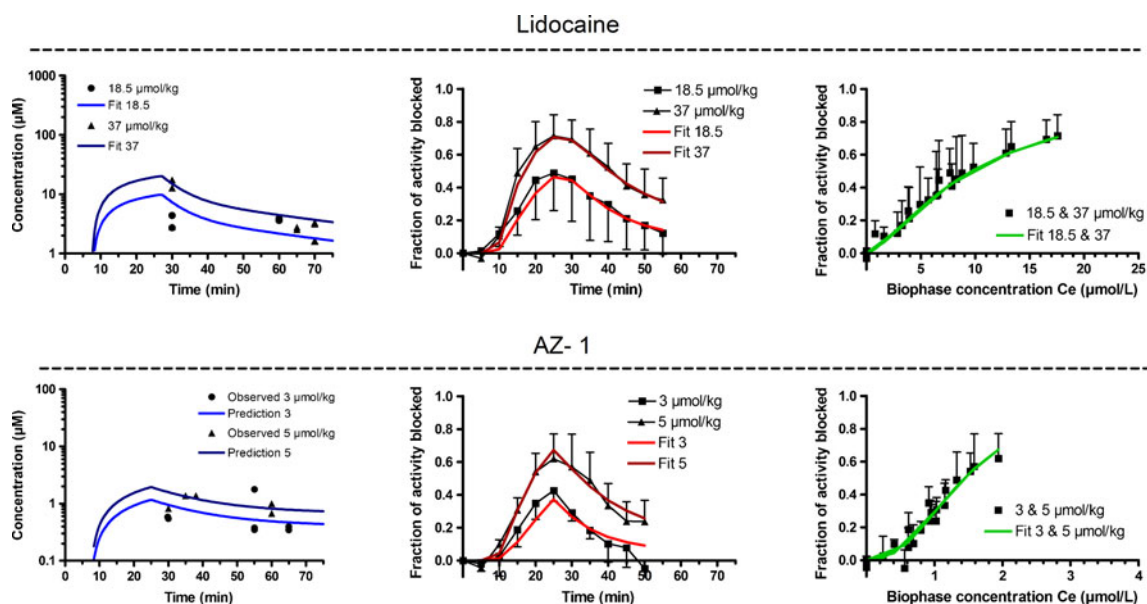


**Fig. 3** *In vivo* electrophysiology observations for 2 sodium channel blockers: Lidocaine and AZ-1. *Left panels*: Observed and fitted plasma concentrations in a simultaneous analysis with additional intravenous PK data (data not shown). *Middle panels*: observed and simultaneously fitted time-course of the inhibition of ectopic activity (mean  $\pm$  SE) at two dose levels. *Right panels*: the relationship between the biophase concentration and the observed and predicted inhibition of ectopic activity. Similar graphs for all other tested additional compounds can be found in the Supplementary Material (S1 and S2).

**Table II** Pharmacodynamic Parameter Estimates of *In Vivo* and *Ex Vivo* Inhibition of Ectopic Activity

Name	<i>In vivo</i> inhibition					<i>Ex vivo</i> inhibition		
	IC <sub>50</sub> [µM]	SE	IC <sub>50,unb</sub> [µM]	Slope	k <sub>eo</sub> [1/h]	EC50 [µM]	SE	Slope
Amitriptyline	1.0	0.1	0.09	1.7	0.07	3	0.2	1.2
Carbamazepine	79	6.0	24	1.5	0.21	21	0.8	2.1
Lamotrigine	10	0.8	5.1	1.8	0.34	22	1.1	1.9
Lidocaine	6.7	0.5	3.9	1.6	0.66	13	1.1	1.1
Mexiletine	13	3.4	5.1	2.4	0.52			
Tetracaine						0.06	0.01	0.8
AZ-1 (a)	1.4	0.1	0.16	2.4	26	0.28	0.02	1.0
AZ-2 (a)	4.3	0.6	0.38	1.4	0.41			
AZ-3 (a)	3.6	0.3	0.28	2.0	32	2.7	0.4	0.8
AZ-4 (a)	2.0	0.2	0.26	1.5	17	0.56	0.1	0.9
AZ-5 (a)	4.0	0.1	0.76	1.0	0.5	1.6	0.3	0.8
AZ-6 (e)	3.6	0.2	0.12	1.3	10 <sup>a</sup>			
AZ-7 (a)						2.4	0.4	0.8
AZ-8 (a)						0.67	0.12	0.7
AZ-9 (b)						1.6	0.1	1.1
AZ-10 (c)						0.62	0.04	1.1
AZ-11 (a)						2.4	0.5	0.7
AZ-12 (a)						0.94	0.1	1.3
AZ-13 (a)						0.83	0.05	1.5
AZ-14 (e)						1.3	0.1	1.5
AZ-15 (e)						0.52	0.03	1.0
AZ-16 (d)						0.32	0.03	2.0
AZ-17 (e)						0.012	0.001	2.2
AZ-18 (f)						3.8	0.4	0.9
AZ-19 (c)						0.84	0.1	1.2
AZ-20 (e)						0.020	0.001	1.4

(a)(21); (b)(19); (c)(20); (d)(22); (e)(23); (f) in house, not published

<sup>a</sup>fixed

the ectopic activity (Fig. 3 right panels). The half-life of distributional delay ( $\ln 2/k_{eo}$ ) ranged between less than 1 min (in-house compounds) to 10 min (amitriptyline). The hill slope ranged between 1 and 2.4 with no difference between in-house compounds and clinically used sodium channel blockers.

### Ex Vivo Electrophysiology

Single fiber *ex vivo* recordings were performed on isolated DRG neurons with ectopic discharges from SNL rats using five clinically used drugs and eighteen experimental compounds. From each SNL rat approximately three isolated DRG neurons with ectopic firing were recorded, and for each compound 7–10 units were analyzed. The averaged basal firing frequency was between 11 and 17 Hz, and similar between all analyzed DRGs. Figure 4 shows the results obtained with lidocaine. A concentration-dependent inhibition was observed in all units following perfusion of 5, 15 and 50  $\mu\text{M}$  of the drug. Buffer perfusion did not significantly affect the frequency of the ectopic discharges. The inhibition of the ectopic activity slowly increased after each new concentration level indicating a delay in the effect. Based on a data analysis of more than ten compounds, this delay in distribution was estimated at 5 min. In the modeling procedure, the delay was therefore fixed at 5 min, which allowed for prediction of the actual concentration in the chamber. The predicted concentrations in the chamber were used as driver of the effect following Eq. 1 for the estimation of the  $IC_{50}$  and  $n$ . Similarly to the *in vivo* data analysis,  $E_{max}$  was fixed at 1 (i.e., full inhibition possible) and  $E_0$  was fixed at 0.

Estimated  $IC_{50}$  values are listed in Table II. The slope values ( $n$ ) ranged from 0.7 to 2.2. Figure 5 shows that the average time-course profiles of the reduction of ectopic discharges in rat DRG by lidocaine and AZ-1 were

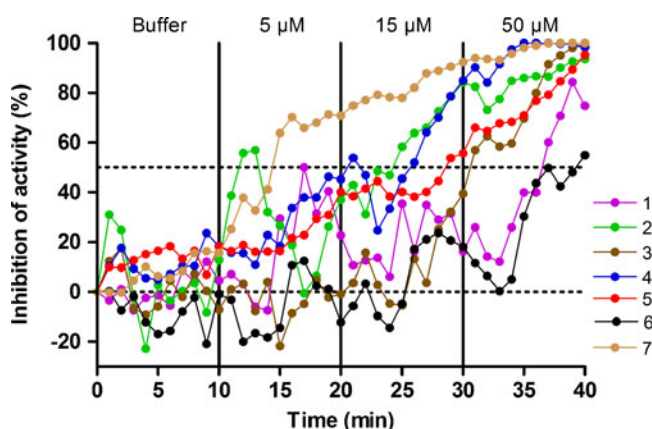


**Fig. 4** Individual recordings for *ex vivo* ectopic activity. Lidocaine in concentrations of 5, 15 and 50  $\mu\text{M}$  was cumulatively applied on DRGs and produced a concentration-dependent inhibition on ectopic discharge.

accurately described by the PKPD model. A full inhibitory curve could be constructed from the concentrations in the biophase from both doses and the inhibitory effect on the ectopic activity (Fig. 5, right panels).

### In Vitro Electrophysiology

*In vitro* potencies for the 26 compounds on the rat and human NaV1.7 channel were determined by automated perforated whole-cell patch clamp using the automated Ion Works instrument with a steady-state protocol ( $V_{\text{hold}}$  -65 mV). Estimation of the state-dependent properties was determined with a resting-state protocol ( $V_{\text{hold}}$  -90 mV).

The generated results are listed in Table III. The compounds covered a potency range with the  $V_{\text{hold}}$  -65 mV protocol of approximately four orders of magnitude, where the clinically used compounds displayed the lowest potencies. The species differences for most compounds was less than 5-fold, with a few exceptions of AZ-2, AZ-7 and AZ-14 that showed up to 16-fold higher potency for the human channel as compared to the rat channel. The potency difference between the resting-state ( $V_{\text{hold}}$  -90 mV) and the steady-state ( $V_{\text{hold}}$  -65 mV) protocols reflected preferential affinity for the inactivated *versus* resting state of the NaV1.7 channel. For the clinically available drugs the difference ranged from 5-fold for tetracaine to 22-fold for lamotrigine. AZ-2, AZ-7 and AZ-19 displayed similar state-dependent properties to lamotrigine, whereas AZ-9, AZ-12, AZ-18 displayed significantly greater degrees of state dependency from 54- to 140-fold. Only two of the tested compounds, AZ-14 and AZ-15, showed less state-dependent properties than tetracaine.

### Correlations

*In vitro* potencies generated in the rat NaV1.7 ( $V_{\text{hold}}$  -65 mV) assay were predictive of the *ex vivo* or *in vivo* inhibition of ectopic activity as demonstrated in the correlations plots shown in Fig. 6. A good correlation ( $R^2=0.85$ ) was observed between the rat NaV1.7 *in vitro*  $IC_{50}$  and the *ex vivo*  $IC_{50}$  (Fig. 6, left panel). Also, a good correlation ( $R^2=0.86$ ) was found between the rat NaV1.7 *in vitro*  $IC_{50}$  and the *in vivo*  $IC_{50}$  based on free plasma concentrations (Fig. 6, right panel). The  $IC_{50, \text{unb}}$  for *in vivo* ectopic activity was 2- to 5-fold more potent than the *in vitro* rat NaV1.7  $IC_{50}$ . Amitriptyline was an exception to this, being 30-fold more potent *in vivo* than *in vitro*. When comparing *ex vivo* and *in vivo* electrophysiology, also a good agreement was found in potencies for the 9 compounds tested, except for amitriptyline, which is 30-fold more potent *in vivo* based on unbound concentrations (see Table II).



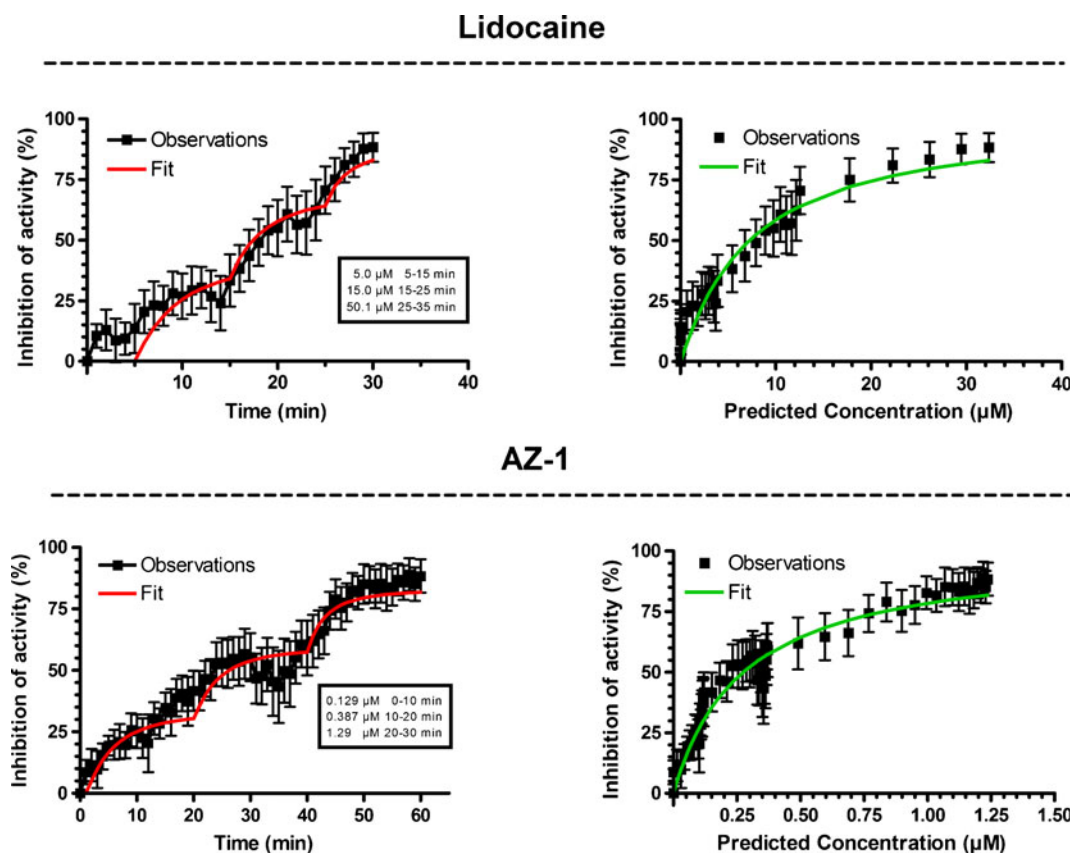


**Fig. 5** *Ex vivo* electrophysiology observations for 2 sodium channel blockers: Lidocaine and AZ-1. *Left panels:* observed and fitted time-course of the inhibition of ectopic activity (mean  $\pm$  SE) during three subsequent applications of (increasing) concentrations. *Right panels:* the relationship between the predicted concentration in the chamber and the observed and predicted inhibition of ectopic activity.

A summary of the generated rat *in vivo* results as well as the reported human data from the literature are shown in Table IV. As shown in Fig. 7, there was an excellent correlation between rat and human *in vitro*. A correlation ( $R^2=0.86$ ) was observed between the *in vitro*  $IC_{50}$  for the rat and human NaV1.7 (left panel). Also *in vivo* a correlation ( $R^2=0.87$ ) was observed between the *in vivo*  $IC_{50}$  based on free concentrations in rats and the unbound clinical effective concentrations (right panel). The mean unbound clinical effective concentrations were within 3-fold of the unbound *in vivo*  $IC_{50}$  in rat, except for carbamazepine. Caution should be exercised though, realizing that the correlation depends much on one compound and that more compounds are needed to validate this relationship. This is further addressed when we discuss the Xenon compound in the discussion.

## DISCUSSION

In the present study, a good agreement was demonstrated between rat and human *in vivo* inhibition of

ectopic activity and therapeutic concentrations for clinically used sodium channel blockers. This suggests that predictions of clinical efficacy for newly developed sodium channel blockers for reducing neuropathic pain could be based on *in vivo* electrophysiology experiments. It was also demonstrated that *in vitro* potency on the NaV1.7 channel correlated well to inhibition of ectopic activity measured *ex vivo* or *in vivo* for clinically used sodium channel blockers and novel more potent NaV1.7 blockers. Therefore, screening and optimization of novel NaV 1.7 blockers could be based on *in vitro* IonWorks data generation. Only the most promising compounds would be required to be characterized in animal models.

## In Vivo Ectopic Activity

Ligation of the spinal nerve in rat is a frequently used preclinical model to study neuropathic pain and results in 4- to 6-fold increase in the incidence of spontaneous ectopic activity in sensory A fibres (30). While the role of specific fibre types involved in the initiation and maintenance of central sensitization in neuropathic

**Table III** *In Vitro* Potency ( $IC_{50}$ ) on Rat and Human NaV1.7 Channels as Measured in the Electrophysiology Assays

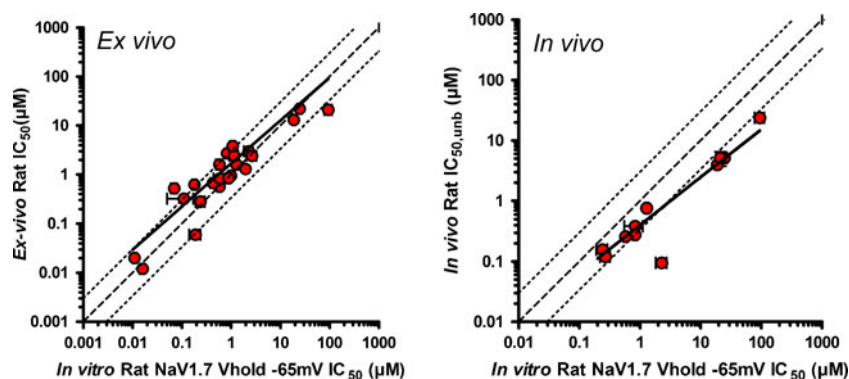
Name	Rat NaV1.7 ( $V_{hold}$ -65 mV)			Human NaV1.7 ( $V_{hold}$ -65 mV)			Human NaV1.7 ( $V_{hold}$ -90 mV)		
	EC50 [ $\mu$ M]	SE	n	EC50 [ $\mu$ M]	SE	n	EC50 [ $\mu$ M]	SE	n
Amitriptyline	2.3	0.47	12	1.1	0.3	12	8.3	1.5	6
Carbamazepine	95	17.0	18	38	7.0	12	327	27	12
Lamotrigine	25	2.4	18	8.1	1.5	12	179	27	12
Lidocaine	19	1.4	16	5.0	0.7	10	63	9	10
Mexiletine	21	2.0	17	11	1.0	8	84	17	10
Tetracaine	0.19	0.05	35	0.11	0.02	41	0.56	0.01	38
AZ-1 (a)	0.24	0.05	16	0.15	0.02	12			
AZ-2 (a)	0.83	0.28	20	0.08	0.01	6	2.0	0.2	6
AZ-3 (a)	0.83	0.07	36	0.16	0.02	34	1.6	0.1	34
AZ-4 (a)	0.58	0.05	16	0.22	0.07	8	1.4	0.4	6
AZ-5 (a)	1.3	0.10	34	0.43	0.06	31	3.2	0.6	13
AZ-6 (e)	0.27	0.05	20	0.13	0.02	29			
AZ-7 (a)	2.7	0.6	12	0.30	0.06	8	6.9	1.4	8
AZ-8 (a)	0.43	0.05	20	0.17	0.02	22	1.4	0.1	22
AZ-9 (b)	0.58	0.09	12	0.12	0.06	6	17	1.3	7
AZ-10 (c)	0.18	0.02	6	0.065	0.020	4	0.16	0.08	3
AZ-11 (a)	1.2	0.2	12	0.53	0.07	16	4.8	1.4	10
AZ-12 (a)	1.0	0.1	32	0.25	0.03	26	14	1.4	21
AZ-13 (a)	0.59	0.15	24	0.17	0.05	23	2.0	0.4	16
AZ-14 (e)	2.0	0.1	4	0.12	0.02	6			
AZ-15 (e)	0.067	0.013	4	0.24	0.05	6	0.18	0.06	4
AZ-16 (d)	0.11	0.06	4	0.16	0.02	4	1.0	0.1	4
AZ-17 (e)	0.016	0.002	8	0.004	0.001	8			
AZ-18 (f)	1.1	0.1	6	0.22	0.03	12	28	2.9	2
AZ-19 (c)	0.89	0.08	8	0.31	0.02	8	5.0	1.3	6
AZ-20 (e)	0.011	0.001	8	0.0025	0.0005	6			

(a)(21); (b)(19); (c) (20); (d)(22); (e) (23); (f) in house, not published

conditions remains controversial (17, 31, 32), emerging evidence suggests that drug-mediated inhibition of aberrant activity of injured A fibres in neuropathic pain models may indicate their therapeutic potential (16, 17, 33, 34). The results described in this paper support these observations. The inhibitory effects on ectopic

activity using the clinically available sodium channel blockers in this study are generally in line with those previously reported on carbamazepine (15, 35), lamotrigine (16), mexiletine (14) and lidocaine (16). Some differences related to the temporal resolution of the effects were observed though. These may be due to

**Fig. 6** Comparison of *in vitro*  $IC_{50}$  vs *ex vivo*  $IC_{50}$  (left) and *in vitro*  $IC_{50}$  vs *in vivo*  $IC_{50}$  (right) in rats. *In vitro* potencies derived in the rat NaV1.7 ionworks assay were predictive of the *ex vivo* or *in vivo* inhibition of ectopic activity suggesting that *in vitro* results can be used for characterization and selection of novel compound without *in vivo* experimentation.



differences in administration schedules, in achieved exposure –not always measured– or the origin of the ectopic activity.

In the present *in vivo* study, recorded units did not show a uniform inhibitory profile upon compound application within one dose group. Such variability in inhibitory responses, which was similar between different compounds and dose levels, might depend on the fraction of available inactivated tetrodotoxin-sensitive sodium channels. Non-selective sodium channel blockers interact predominantly with the inactivated state of the channels and these specific interactions are thought be the most pharmacologically relevant (36). The differential expression of these channels, together with channel functional properties including channel phosphorylation, probability of channel opening, the mean channel open time or unitary channel conductance (31) might explain, at least partly, the different level of susceptibility of the various spontaneously active axons to applied agents.

### Correlations to *In Vitro* and *Ex Vivo* Electrophysiology

*In vitro* potency of sodium channel blockers depends mostly on the used protocol, but also on the expression system and the instrument platform used for the analysis. The majority of sodium channel blockers display state-dependent properties, where the degree of state-dependency can be more than 100-fold, as shown here. Frequency and use dependence are other well-known attributes of sodium channel blockers. Examples of compounds that display such properties are e.g., tetracaine, whereas e.g., lamotrigine, as well as AZ-3, show no frequency and use dependent properties (37) and data on file. Ion channel drug discovery has until recently been hampered by the slow throughput of available instrumentation. Platforms like the IonWorks Quattro system have revolutionized the ability to generate electrophysiological data (25). However, there are several differences between how compounds are being analysed by this system compared to classical patch-clamp electrophysiology. Some of the main differences include discontinuous voltage control, and a fairly long incubation time, which is ~3 min in the used assay. For some compounds the potencies are significantly reduced, whereas other compounds show no change in potency when analysed with similar protocols using manual patch-clamp as compared to Ion Works Quattro (unpublished results). The reasons behind this remain to be elucidated.

The good correlation between the *in vitro* and *in vivo* potencies of all examined sodium channel blockers demonstrates clearly the relevance of the used steady-state

( $V_{\text{hold}} -65$  mV) assay. The studied clinically used sodium channel blockers were 2–5 fold more potent *in vivo* compared to the *in vitro* NaV1.7 channel potency. The observation that more potent and potentially more selective NaV1.7 inhibitors show a similar *in vitro-in vivo* correlation as the clinically used sodium channel blockers also suggests that block of the aberrant neuronal firing occurs mainly via NaV1.7 channel block in rat. As shown here, the ability to predict the *in vivo* pharmacological outcome, together with early pharmacokinetic analysis, could strongly reduce the need of preclinical *in vivo* efficacy screening studies in a NaV1.7 drug discovery program.

Out of the six clinically available compounds lidocaine has been studied previously by *ex vivo* electrophysiology. In the present study, inhibition of SNL-induced ectopic activity was achieved with an  $IC_{50}$  of 13  $\mu\text{M}$  (Table II). Previously, a 30% inhibition was seen with the compound when applied at 9.3 and 18.5  $\mu\text{M}$  on a similar DRG preparation, without block of nerve conduction (24), indicating a good agreement between the two studies. In addition, our findings are in line with previous studies that the ectopic discharges generator mechanisms lie mainly within the DRG (24, 38, 39).

### Pharmacokinetic-Pharmacodynamic Translational Approach

To our knowledge, this is the first study that used a PKPD approach to evaluate compound effects on aberrant neuronal activity. In this approach, the time-course of the ectopic activity and the drug exposure are integrated to be able to derive an *in vivo* potency value. It was shown that a short delay between plasma concentrations and effect was observed. This delay could be either caused by a distributional delay of the compound to the site of action (29), an indirect response to the inhibition of the channel (40), or a reflection of a difference between on- and off-rate on the channel (41). The underlying cause of this observed delay cannot univocally be derived from these data, but require further investigation. However, to derive the accurate  $IC_{50}$  estimates it is necessary to take these delays into account using PKPD modelling. Advantage of using a mathematical PKPD model to describe the effects is that this allows for predictions of ectopic activity under different conditions, such as different doses or infusion rates. This becomes particularly important in the early drug development setting, in which predictions need to be made for expected efficacy profiles for new chemical entities in early clinical testing.

In this investigation there was a good agreement between rat and human for clinically used sodium

**Table IV** Comparison of *In Vivo* Inhibitory Potency in Rats Based on the *In Vivo* Electrophysiology and the Clinical Effective Concentration Range, Both Corrected for Plasma Protein Binding

Compound	Rat			Human		
	$IC_{50}$ ( $\mu$ M)	$f_u$ rat	$IC_{50,unb}$ ( $\mu$ M)	Clinical $C_{eff}$ ( $\mu$ M)	$f_u$ human	$C_{eff,unb}$ ( $\mu$ M)
Amitriptyline	1.0	0.09	0.09	0.2–0.8 <sup>a</sup>	0.07	0.01–0.05
Carbamazepine	79	0.30	24	10–30 <sup>b</sup>	0.25	2.5–7.5
Lamotrigine	10	0.51	5.1	10–25 <sup>c</sup>	0.55	5.5–14
Lidocaine	9.6	0.59	5.4	5–15 <sup>d</sup>	0.35	1.8–5.3
Mexiletine	13	0.74	9.6	3–11 <sup>e</sup>	0.65	2–7.2

<sup>a</sup> Leijon G et al., Pain 1989 Jan;36(1):27–36.; Pilowsky I et al., Pain 1982 Oct;14(2):169–179.; Max MB et al., N Engl J Med 1992 May 7;326(19):1250–1256

<sup>b</sup> Graves NM et al., Epilepsia 1985 Sep–Oct;26(5):429–433; Wada JA et al., Epilepsia 1978 Jun;19(3):251–255. Morselli PL et al., Epilepsia 1975 Dec;16(5):759–764. Lindstrom P et al., Pain 1987 Jan;28(1):45–50

<sup>c</sup> Finnerup NB et al., Pain 2002 Apr;96(3):375–383; Lunardi G et al., Neurology 1997 Jun;48(6):1714–1717

<sup>d</sup> Boas RA et al., Br J Anaesth 1982 May;54(5):501–505; Galer BS et al., J Pain Symptom Manage 1996 Sep;12(3):161–167; Wallace MS et al., Anesthesiology 2000 Jan;92(1):75–83

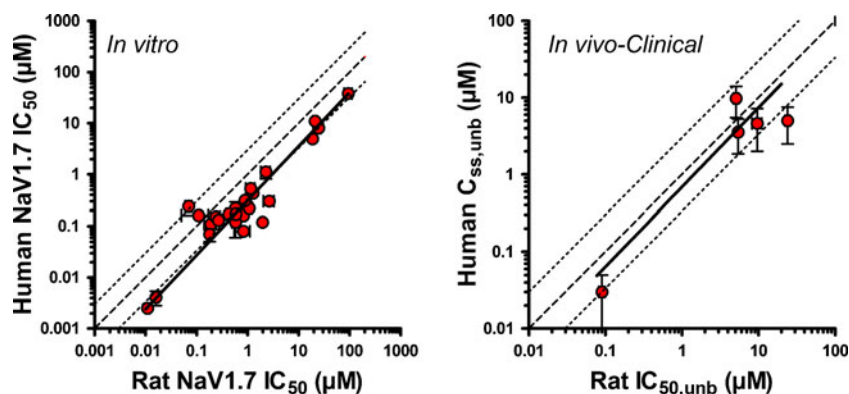
<sup>e</sup> Deigard A et al., Lancet 1988 Jan 2–9;1(8575–6):9–11; Nathan A et al., Pediatrics 2005 Apr;115(4):e504–7

channel blockers with regards to the unbound clinically effective concentration and the unbound concentrations inhibiting ectopic activity in rats with 50%. Together with the good agreement with *in vitro* potencies on the rat and human NaV1.7 channels, these data further strengthen the indicated important role of the NaV1.7 channel in pain perception and that inhibitory effects of test compounds on aberrant activity of injured A fibres in neuropathic pain models may indicate their therapeutic potential (16, 17, 33, 34). Interestingly, amitriptyline was 30–40-fold more potent *in vivo* and clinically compared to the *in vitro* potency. This exception might indicate that amitriptyline has a high susceptibility of towards TTX-sensitive channels involved in the maintenance of the ectopic activity *in vivo*, which is not accounted for *in vitro*. Besides, this would indicate that additional mechanisms of action contribute to the clinical effects of amitriptyline in neuropathic pain both in rat and human. It is known that amitriptyline interacts

with norepinephrine and/or serotonin reuptake, and a wide spectrum of receptors such as histamine, opiate, NMDA and adenosine receptors (36).

Taken together, these results increased the confidence in the usefulness of the applied animal model to predict clinical efficacy of more selective sodium channel blockers. This could be done by comparing the *in vitro* and *in vivo* profile of these more selective sodium channel blockers to existing non-selective blockers and extrapolate these observations to the putative clinical efficacy profile based on the predicted human pharmacokinetics (42). An interesting compound to test the predictivity of the *in vivo* SNL model is the NaV1.7 blocker XEN402 (reported  $IC_{50}$  80 nM). In recently disclosed results from an exploratory clinical trial it was shown that attenuated pain perception in mutation-proven erythromelalgia patients following a dose regimen of 400 mg orally twice daily (43). Unfortunately, no pharmacokinetic data has been disclosed, which prevents the evaluation of the human effective concentration for XEN402 in the context of this study.

**Fig. 7** Comparison of rat and human *in vitro*  $IC_{50}$  (left panel) and correlation between *in vivo* and clinical effective unbound plasma concentrations in rat and human. There was an excellent agreement with rat and human both *in vitro* and *in vivo* suggesting that *in vivo* inhibition of ectopic activity could be used for prediction of clinically effective concentrations for novel NaV compounds.



## CONCLUSION

In conclusion, it was demonstrated that inhibition of ectopic activity in the SNL pain model occurred at similar free concentration levels as clinical effective concentrations in humans. Together with a good correlation between the rat and human Nav1.7 channel, this suggests that *in vivo*  $IC_{50}$  could be used for human dose projections for clinical effects of new more selective sodium channel blockers. In addition, the good correlation between *in vitro* and *in vivo* electrophysiology is supportive of using *in vitro* potency for early characterization and selection of novel sodium channel blockers, thereby reducing the need for *in vivo* testing. The validity of this approach cannot be completely evaluated until detailed clinical data with the first selective Nav1.7 blocker becomes available.

## ACKNOWLEDGMENTS AND DISCLOSURES

The authors would like to thank Vibeke Tæpp for technical help regarding the preparation of the animal model and Sveinn Briem and Yvonne Jaksch for their help with the bioanalysis of plasma and protein binding samples.

## REFERENCES

1. Dray A. Neuropathic pain: emerging treatments. *Br J Anaesth*. 2008;101(1):48–58.
2. Priest BT, Kaczorowski GJ. Blocking sodium channels to treat neuropathic pain. *Expert Opin Ther Targets*. 2007;11(3):291–306.
3. Bhattacharya A, Wickenden AD, Chaplan SR. Sodium channel blockers for the treatment of neuropathic pain. *Neurotherapeutics*. 2009;6(4):663–78.
4. Krafft DS, Bannan AW. Sodium channels and nociception: recent concepts and therapeutic opportunities. *Curr Opin Pharmacol*. 2008;8(1):50–6.
5. Cox JJ, Reimann F, Nicholas AK, Thornton G, Roberts E, Springell K, *et al*. An SCN9A channelopathy causes congenital inability to experience pain. *Nature*. 2006;444(7121):894–8.
6. Ahmad S, Dahllund L, Eriksson AB, Hellgren D, Karlsson U, Lund PE, *et al*. A stop codon mutation in SCN9A causes lack of pain sensation. *Hum Mol Genet*. 2007;16(17):2114–21.
7. Cummins TR, Dib-Hajj SD, Waxman SG. Electrophysiological properties of mutant Nav1.7 sodium channels in a painful inherited neuropathy. *J Neurosci*. 2004;24(38):8232–6.
8. Fertleman CR, Baker MD, Parker KA, Moffatt S, Elmslie FV, Abrahamsen B, *et al*. SCN9A mutations in paroxysmal extreme pain disorder: allelic variants underlie distinct channel defects and phenotypes. *Neuron*. 2006;52(5):767–74.
9. Attal N, Bouhassira D. Translating basic research on sodium channels in human neuropathic pain. *J Pain*. 2006;7(1 Suppl 1):S31–7.
10. Dib-Hajj SD, Black JA, Waxman SG. Voltage-gated sodium channels: therapeutic targets for pain. *Pain Med*. 2009;10(7):1260–9.
11. Gabrielsson J, Dolgos H, Gillberg PG, Bredberg U, Benthem B, Duker G. Early integration of pharmacokinetic and dynamic reasoning is essential for optimal development of lead compounds: strategic considerations. *Drug Discov Today*. 2009;14(7–8):358–72.
12. Krekels EH, Angesjo M, Sjogren I, Moller KA, Berge OG, Visser SA. Pharmacokinetic-pharmacodynamic modeling of the inhibitory effects of naproxen on the time-courses of inflammatory pain, fever, and the *ex vivo* synthesis of TXB2 and PGE2 in rats. *Pharm Res*. 2011;28(7):1561–76.
13. Van Der Graaf PH, Gabrielsson J. Pharmacokinetic-pharmacodynamic reasoning in drug discovery and early development. *Future Med Chem*. 2009;1(8):1371–4.
14. Nakamura S, Atsuta Y. Effect of sodium channel blocker (mexiletine) on pathological ectopic firing pattern in a rat chronic constriction nerve injury model. *J Orthop Sci*. 2005;10(3):315–20.
15. Yates JM, Smith KG, Robinson PP. The effect of carbamazepine on injury-induced ectopic discharge in the lingual nerve. *Brain Res*. 2005;1051(1–2):1–7.
16. Ritter AM, Ritchie C, Martin WJ. Relationship between the firing frequency of injured peripheral neurons and inhibition of firing by sodium channel blockers. *J Pain*. 2007;8(4):287–95.
17. Su X, Liang AH, Urban MO. The effect of amitriptyline on ectopic discharge of primary afferent fibers in the L5 dorsal root in a rat model of neuropathic pain. *Anesth Analg*. 2009;108(5):1671–9.
18. Kirillova I, Teliban A, Gorodetskaya N, Grossmann L, Bartsch F, Rausch VH, *et al*. Effect of local and intravenous lidocaine on ongoing activity in injured afferent nerve fibers. *Pain*. 2011;152(7):1562–71.
19. Macsari I, Sandberg L, Besidski Y, Gravenfors Y, Ginman T, Bylund J, *et al*. Phenyl isoxazole voltage-gated sodium channel blockers: structure and activity relationship. *Bioorg Med Chem Lett*. 2011;21(13):3871–6.
20. Kers I, Macsari I, Csajernyk G, Nylof M, Skogholm K, Sandberg L, *et al*. Phenethyl nicotinamides, a novel class of Na(V)1.7 channel blockers: structure and activity relationship. *Bioorg Med Chem Lett*. 2012;22(19):6108–15.
21. Kers I, Csajernyk G, Macsari I, Nylof M, Sandberg L, Skogholm K, *et al*. Structure and activity relationship in the (S)-N-chroman-3-ylcarboxamide series of voltage-gated sodium channel blockers. *Bioorg Med Chem Lett*. 2012;22(17):5618–24.
22. Macsari I, Besidski Y, Csajernyk G, Nilsson LI, Sandberg L, Yngve U, *et al*. 3-Oxoisoindoline-1-carboxamides: Potent, State-Dependent Blockers of Voltage-Gated Sodium Channel Na(V)1.7 with Efficacy in Rat Pain Models. *J Med Chem*. 2012;55(15):6866–80.
23. Beaudoin S, Laufer-Sweiler MC, Markworth CJ, Marron BE, Millan DS, Rawson DJ. Sulfonamide derivatives. 2010. [Patent].
24. Liu X, Zhou JL, Chung K, Chung JM. Ion channels associated with the ectopic discharges generated after segmental spinal nerve injury in the rat. *Brain Res*. 2001;900(1):119–27.
25. Schroeder K, Neagle B, Trezise DJ, Worley J. Ionworks HT: a new high-throughput electrophysiology measurement platform. *J Biomol Screen*. 2003;8(1):50–64.
26. Bueters T, Dahlstrom J, Kvalvagnaes K, Betner I, Briem S. High-throughput analysis of standardized pharmacokinetic studies in the rat using sample pooling and UPLC-MS/MS. *J Pharm Biomed Anal*. 2011;55(5):1120–6.
27. Briem S, Martinsson S, Bueters T, Skoglund E. Combined approach for high-throughput preparation and analysis of plasma samples from exposure studies. *Rapid Commun Mass Spectrom*. 2007;21(13):1965–72.
28. Borgegård T, Minidis A, Jureus A, Malmberg J, Rosqvist S, Gruber S, *et al*. In vivo analysis using a presenilin-1-specific inhibitor: presenilin-1-containing g-secretase complexes mediate the majority of CNS Ab production in the mouse. *Alzheimer's Dis Res J*. 2011;3(1):30–45.
29. Sheiner LB, Stanski DR, Vozeh S, Miller RD, Ham J. Simultaneous modeling of pharmacokinetics and pharmacodynamics: application to d-tubocurarine. *Clin Pharmacol Ther*. 1979;25(3):358–71.
30. Liu X, Eschenfelder S, Blenk KH, Janig W, Habler H. Spontaneous activity of axotomized afferent neurons after L5 spinal nerve injury in rats. *Pain*. 2000;84(2–3):309–18.



31. Devor M. Ectopic discharge in Abeta afferents as a source of neuropathic pain. *Exp Brain Res*. 2009;196(1):115–28.
32. Gold MS. Spinal nerve ligation: what to blame for the pain and why. *Pain*. 2000;84(2–3):117–20.
33. Pan HL, Eisenach JC, Chen SR. Gabapentin suppresses ectopic nerve discharges and reverses allodynia in neuropathic rats. *J Pharmacol Exp Ther*. 1999;288(3):1026–30.
34. Abdi S, Lee DH, Chung JM. The anti-allodynic effects of amitriptyline, gabapentin, and lidocaine in a rat model of neuropathic pain. *Anesth Analg*. 1998;87(6):1360–6.
35. Burchiel KJ. Carbamazepine inhibits spontaneous activity in experimental neuromas. *Exp Neurol*. 1988;102(2):249–53.
36. Dick IE, Brochu RM, Purohit Y, Kaczorowski GJ, Martin WJ, Priest BT. Sodium channel blockade may contribute to the analgesic efficacy of antidepressants. *J Pain*. 2007;8(4):315–24.
37. Tao H, Guia A, Xie B, Santaana D, Manalo G, Xu J, *et al*. Efficient characterization of use-dependent ion channel blockers by real-time monitoring of channel state. *Assay Drug Dev Technol*. 2006;4(1):57–64.
38. Liu CN, Wall PD, Ben-Dor E, Michaelis M, Amir R, Devor M. Tactile allodynia in the absence of C-fiber activation: altered firing properties of DRG neurons following spinal nerve injury. *Pain*. 2000;85(3):503–21.
39. Liu X, Chung K, Chung JM. Ectopic discharges and adrenergic sensitivity of sensory neurons after spinal nerve injury. *Brain Res*. 1999;849(1–2):244–7.
40. Dayneka NL, Garg V, Jusko WJ. Comparison of four basic models of indirect pharmacodynamic responses. *J Pharmacokinet Biopharm*. 1993;21(4):457–78.
41. Shimada S, Nakajima Y, Yamamoto K, Sawada Y, Iga T. Comparative pharmacodynamics of eight calcium channel blocking agents in Japanese essential hypertensive patients. *Biol Pharm Bull*. 1996;19(3):430–7.
42. Visser SAG, Kalezic I, Luo L, Bueters T, Besidski Y, Nyström JE, *et al*. Pharmacokinetic-pharmacodynamic validation of *in vivo* and *ex vivo* electrophysiology markers for NaV1.7 inhibition in spinal nerve injured rats. In: Danhof M, Van der Graaf PH, Holford N, editors. *Advances in simultaneous pharmacokinetic-pharmacodynamic modelling*; 2010. p. 111–113. [Contribution to a Book].
43. Goldberg YP, Price N, Namdari R, Cohen CJ, Lamers MH, Winters C, *et al*. Treatment of Na(v)1.7-mediated pain in inherited erythromelalgia using a novel sodium channel blocker. *Pain*. 2012;153(1):80–5.